Published in final edited form as:
Integr Biol (Camb). 2012 September 21; 4(9): 1049–1058. doi:10.1039/c2ib20083j.

Soft microenvironments promote the early neurogenic differentiation but not self-renewal of human pluripotent stem cells

Albert J. Keung[1], **Prashanth Asuri**[1,4], **Sanjay Kumar**[2], and **David V. Schaffer**[1,2,3]

[1]Department of Chemical and Biomolecular Engineering, University of California, Berkeley, CA, 94720, USA

[2]Department of Bioengineering, University of California, Berkeley, CA, 94720, USA

[3]Helen Wills Neuroscience Institute, University of California, Berkeley, CA, 94720, USA

Abstract

Human pluripotent stem cells (hPSCs) are of great interest in biology and medicine due to their ability to self-renew and differentiate into any adult or fetal cell type. Important efforts have identified biochemical factors, signaling pathways, and transcriptional networks that regulate hPSC biology. However, recent work investigating the effect of biophysical cues on mammalian cells and adult stem cells suggests that the mechanical properties of the microenvironment, such as stiffness, may also regulate hPSC behavior. While several studies have explored this mechanoregulation in mouse embryonic stem cells (mESCs), it has been challenging to extrapolate these findings and thereby explore their biomedical implications in hPSCs. For example, it remains unclear whether hPSCs can be driven down a given tissue lineage by providing tissue-mimetic stiffness cues. Here we address this open question by investigating the regulation of hPSC neurogenesis by microenvironmental stiffness. We find that increasing extracellular matrix (ECM) stiffness *in vitro* increases hPSC cell and colony spread area but does not alter self-renewal, in contrast to past studies with mESCs. However, softer ECMs with stiffnesses similar to that of neural tissue promote the generation of early neural ectoderm. This mechanosensitive increase in neural ectoderm requires only a short 5-day soft stiffness "pulse," which translates into downstream increases in both total neurons as well as therapeutically relevant dopaminergic neurons. These findings further highlight important differences between mESCs and hPSCs and have implications for both the design of future biomaterials as well as our understanding of early embryonic development.

*Address correspondence to: David V. Schaffer, 274 Stanley Hall, University of California at Berkeley, Berkeley, CA 94720-3220. Tel.: 510-643-5963; Fax: 510-642-4778; schaffer@berkeley.edu, http://www.cchem.berkeley.edu/schaffer/. Sanjay Kumar, 274A Stanley Hall, University of California at Berkeley, Berkeley, CA 94720-3220. Tel.: 510 643-0787, Fax: 510 642-5835, skumar@berkeley.edu, http://kumarlab.berkeley.edu.

[4]Current affiliation: Bioengineering Program, Santa Clara University

Insight Statement

This paper *integrates* physical and material science technologies, including polymeric hydrogel synthesis and mechanical characterization using atomic force microscopy, with a complex biological system of human pluripotent stem cells (hPSC). The *innovative* use of these technologies to study the mechanosensitivity of hPSC self-renewal and neuralization into therapeutically relevant dopaminergic neurons provides indispensible quantitative control of the stiffness of the stem cell microenvironment. These technologies enable this paper's biological *insights*, demonstrating for the first time that hPSC neuralization is mechanosensitive at early temporal periods while self-renewal is not.

Introduction

Human pluripotent stem cells (hPSCs) – including both human embryonic stem cells (hESCs) and human induced pluripotent stem cells (hiPSCs) – hold considerable promise as cell sources for biomedical therapies, disease models, and fundamental biological studies. Recent advances in culture systems[1] as well as in cellular reprogramming[2] have greatly accelerated progress towards many of these goals. For example, dopaminergic neurons, the predominant cell type lost in Parkinson's Disease, have been effectively generated from hPSCs[1, 3] and functionally integrated into animal models[1b], with promise for the development of cell replacement therapies. Clearly, improving our understanding of how the defining properties of self-renewal and differentiation are regulated in both hESCs and hiPSCs will improve the quantity and quality of hPSC-derived, therapeutically relevant cell populations as well as deepen our understanding of organismal development.

Over the past two decades, researchers have assembled considerable knowledge of how biochemical factors, signaling pathways, and transcriptional networks[4] regulate hPSC behaviors. At the same time, it has also become clear that the biophysical properties of the microenvironment, especially extracellular matrix (ECM) stiffness, can powerfully control a variety of cell behaviors, including the self-renewal and differentiation properties of adult stem cells[5]. However, our understanding of how these biophysical inputs may regulate hPSC biology and be leveraged to drive differentiation into therapeutically desirable cell types remains in its infancy. Previous work in mouse embryonic stem cells (mESCs) suggests that biophysical cues such as cyclic strain or stiffness[6] may be important in regulating cell behavior. However, hPSCs exhibit starkly different behaviors from mESCs, including their colony-based growth, sensitivity to different growth factors[7], and response to the biophysical cues of cyclic strain[8]. These findings are consistent with early observations of differential marker expression[9] as well as recent sequencing efforts that have revealed substantial transcriptomic differences between mESCs and hESCs and only modest overlap between pathways critical for self-renewal in each species[10]. Thus, due to these overall differences between mESCs and hPSCs, phenomenology obtained with mESCs cannot be assumed *a priori* to hold for hPSCs. Furthermore, standard hPSC culture systems are more complex than those for mESCs. For example, hPSC culture requires either co-culture with feeder cells or matrix proteins, such as in the highly complex product Matrigel, instead of simple collagen coated surfaces. Moreover, hPSCs must be cultured as colonies due to the low survival of dissociated single hPSCs. This relative complexity of hPSC compared to mESC culture may explain why comparatively little is known about hPSC mechanobiology. Given the intense interest in biomaterials development for hPSC cultures[11], it is important to understand how biophysical regulatory aspects of the microenvironment could be leveraged to create highly defined culture systems for hPSCs.

To study the effect of microenvironmental stiffness in isolation from other potentially confounding factors, hESC and hiPSC colonies were cultured on Matrigel-coated polyacrylamide gels and found to increase in cell and colony spread area with increasing extracellular matrix (ECM) stiffness. However, hPSC self-renewal was not affected, in contrast to previous findings with mESCs. Interestingly, using an adherent differentiation protocol[1a] in which cells experience the mechanical properties of the biomaterial substrate, softer ECMs were found to promote both hESC and hiPSC differentiation into neurons and subsequently into therapeutically relevant dopaminergic neurons. Furthermore, by analyzing early neural ectodermal marker expression as well as by shortening the temporal exposure to soft ECM stiffnesses, hESCs and hiPSCs were found to be mechanically responsive at an early period during differentiation. These results expand our understanding of hPSC developmental biology and identify a new biophysical axis of control to improve the generation of therapeutically relevant dopaminergic neurons.

Results

hPSC cell and colony area increase with ECM stiffness

We first sought to ask whether microenvironmental stiffness altered hPSC morphology, self-renewal capacity, and pluripotency. Therefore, hESC and hiPSC colonies were dissociated to 25–50 cell clusters and seeded at equal cell density on 100, 700, and 75000 Pa polyacrylamide ECMs. After 3 days in growth conditions, 4X phase images were acquired (Figure 1, right), and hPSC colony area was quantified (Figure 1, left). Raising ECM stiffness from 100 to 700 Pa and from 100 to 75000 Pa dramatically increased colony area for both hESCs and hiPSCs by about 3-fold and 7-fold.

Since the total number of colonies per cell culture surface area did not change substantially with substrate stiffness (Figure S1), this rise in colony area may be due to either greater cell proliferation or a larger degree of cell spreading on stiff ECMs. To test these possibilities, cultures were dissociated after 3 days in growth conditions, and cell number was quantified by hemocytometer. The overall cell density did not vary with ECM stiffness (Figure 2A), revealing that proliferation was not affected by ECM stiffness and instead indicating that cells on softer ECMs had smaller projected areas within colonies, also observed through phase images (Figure 1, right). In addition, flow cytometry analysis showed that regardless of stiffness, the expression of the pluripotency markers Nanog, Oct-3/4, and SSEA-4 expression were maintained at high levels (Figure 2B). Furthermore, while soft ECMs can maintain mouse embryonic stem cell pluripotency even in the absence of growth factors[6a], hPSCs did not exhibit differences in Tra-1-60 marker expression as a function of ECM stiffness when the growth factors (FGF-2 and TGF-β for hESC, mTeSR supplement for hiPSC) were removed (Figure 2C). Therefore, while hPSC colony morphology was mechanosensitive, cell proliferation and pluripotency were apparently insensitive to ECM stiffness.

Soft ECMs promote early neural ectodermal and neuronal differentiation

Since ECM stiffness did not affect hPSC pluripotency and proliferation, we analyzed whether it modulated differentiation. Substrates with stiffnesses near that of brain tissue (such as 100 and 700 Pa used in this study) have been shown to regulate the behaviors of partially and fully differentiated cells, including adult neural stem cell (aNSC) differentiation[12] and neuronal morphology[13]. We hypothesized that ECM stiffnesses in the 100–700 Pa range may also regulate earlier processes in neural differentiation, such as the generation of neural ectoderm, and hPSCs offer a model to study such early human developmental processes. To address this question, a recent adherent protocol for the generation of neural populations from hPSCs[1a] was adapted by differentiating hESCs and hiPSCs for 9 days on ECMs of different stiffnesses (within the 12-day limit for the reliable stability of the polyacrylamide ECM coatings). 25–50 hPSC clusters were seeded on 100, 700, and 75000 Pa ECMs and cultured in growth conditions for 3 days. Next, to induce differentiation, cells were cultured in Smad inhibitors and KSR for 5 days, followed by the early initiation of dopaminergic neuronal patterning by Sonic hedgehog addition for a subsequent 4 days. Immunostaining (Figures 3C and 3F) showed that 100 Pa ECMs promoted PAX6 positive (neural ectoderm) cell generation at levels 15–20% greater than 700 and 75000 Pa ECMs (Figures 3A and 3D). In addition, consistent with this early stage of differentiation, PAX6 levels were high and comparatively fewer neurons were observed[1a]. However, both 100 and 700 Pa ECMs interestingly promoted TUJ1 positive (neuron) cell generation at levels 2–3 fold greater than 75000 Pa ECMs (Figures 3B and 3E).

Quantitative reverse transcription polymerase chain reaction (QRT-PCR) analysis, conducted to complement the immunostaining, further demonstrated that 100 Pa substrates promoted PAX6 expression (Figure 4A), and both 100 and 700 Pa ECMs promoted TUJ1 induction over 75000 Pa ECMs and polystyrene (Figure 4B) after 9 days of differentiation. We next assessed whether the expression of another early ectodermal precursor marker, such as SOX1, may correlate with PAX6 and in particular TUJ1 positive cells on both 100 and 700 Pa ECMs. Interestingly, the early ectodermally expressed SOX1 tracked TUJ1 expression, with greater expression on both 100 and 700 Pa ECMs compared to 75000 Pa ECMs and polystyrene (Figure 4C). These results indicated that ECM stiffness modulates early neural differentiation events and therefore offers the potential to increase subsequent neuronal differentiation.

Soft ECMs promote dopaminergic and overall neuronal differentiation

We next determined whether the higher levels of neural differentiation observed on soft substrates after 9 days translate to downstream increases in the number of mature neurons, particularly dopaminergic neurons. hPSCs were cultured for 9 days on 100, 700, 75000 Pa ECMs or polystyrene as before, passaged *en bloc* to glass chamber wells for an additional 10 days to allow for neuronal maturation, and analyzed for the number of TUJ1 positive neurons and tyrosine hydroxylase (TH) positive dopaminergic neurons. The proportion of neurons within the culture progressively increased with decreasing ECM stiffness for both hESCs (Figures 5A, 5B, and 5D) and hiPSCs (Figures 5E, 5F, and 5H), with slightly lower numbers for hiPSCs. Furthermore, the fraction of these neurons that were TH+ did not change with stiffness, suggesting ECM stiffness may act primarily during early differentiation processes into early neural ectoderm/progenitors and not during neural patterning; however, the yield of TH positive cells increased with softer materials since the number of neurons increased. In sum, the proportion of TUJ1 and TH positive cells are nearly 3-fold higher on soft ECMs compared to traditional polystyrene ECMs.

Only a brief 5 day exposure to soft ECMs is required to increase dopaminergic differentiation

SOX1 expression has been shown to plateau after 5 days in Smad-inhibiting conditions[1a]. Therefore, ECM stiffness may modulate SOX1 expression (Figure 4C) by regulating early differentiation processes prior to the addition of neural patterning factors on day 5 (Figure 6A). Furthermore, the percentage of dopaminergic over total neurons is invariant with ECM stiffness (Figure 5C and 5G), indicating that ECM stiffness exerts less influence from days 5–9, the first days of neural patterning when dopaminergic specification would begin to occur. We therefore asked if cells cultured on different ECM stiffnesses for less time (5 rather than 9 days) could still enjoy the full effects of ECM stiffness on the final dopaminergic neuron levels (Figure 6A). When this “stiffness pulse” window was decreased to the first 5 days of differentiation, 700 Pa ECMs still promoted neuronal and dopaminergic neuronal differentiation over 75000 Pa ECMs (Figure 6B, 6C, 6F, and 6G) and importantly yielded similar percentages of each cell type as with the longer 9 day pulse (Figure 5). Thus, ECM stiffness operated primarily during initial differentiation into neural ectoderm and exerted less influence during the subsequent neural patterning.

Discussion

We have shown that ECM stiffness regulates early differentiation but not self-renewal of hPSCs. In particular, while hPSC morphology is mechanosensitive under growth conditions, since cell and colony areas increase with increasing ECM stiffness, pluripotency marker expression and cell proliferation are not affected by ECM stiffness. In contrast, early neurogenic differentiation into SOX1 positive neural ectoderm prior to neural patterning is

strongly modulated by this biophysical input. After further neural patterning and maturation, this effect translates to higher percentages of total neurons as well as dopaminergic neurons.

The relative stiffness-insensitivity of hPSC pluripotency marker expression contrasts with the observed rescue of mESC pluripotency on soft ECMs in the absence of growth factors[6a]. In fact, while Tra-1-60 expression did not decrease significantly for the MSC-iPS upon growth factor withdrawal as it did for the H1 cells (likely due to differences in basal mTeSR versus X-VIVO media conditions), neither culture survived past 6 days in the absence of growth factors regardless of substrate stiffness. These results suggest that continued investigations into ESCs derived from both species will be needed to develop a more complete picture of the nature of pluripotency. These species-dependent differences are consistent with past comparative observations between hPSCs and mESCs. For example, these two cell types have exhibited differing responses to another biophysical cue, cyclic strain, which was shown to inhibit human ESC[8] but promote mouse ESC[6b] differentiation. These contrasting mechanosensitive phenotypes may arise from a growing list of observed differences in the fundamental cell biology of human and mouse ESCs, including in developmental stage[14], transcription factor binding[15], pluripotency marker expression[16], nuclear receptor expression during differentiation[17], keratin expression[18], and growth factors and signaling pathways that maintain pluripotency[19]. In the future it may be interesting to compare potential crosstalk between these numerous factors and candidate mechanotransductive signaling pathways[5c, 20] to elucidate species-distinct mechanosensitive behaviors and to understand biomedically relevant, human-specific properties that could be harnessed for therapeutic application.

Our finding that hiPSCs, like adult NSCs[5c, 12], increase neurogenesis on softer substrates offers important implications for the future development of biomedical therapies. hiPSCs in particular hold promise for patient-specific cell replacement therapies since they may more effectively evade immune responses than allogeneic hESC grafts, as well as bypass potential ethical concerns and corresponding supply limitations of embryo-derived hESCs in some countries. hiPSCs did exhibit lower overall levels of neurogenesis compared to hESCs, potentially due to epigenetic memory of their mesenchymal origins[21]. However, the fact that hiPSC neural differentiation was still mechanosensitive despite epigenetic and transcriptomic differences between hiPSCs and hESCs[22] and significantly different methods of derivation[2a, 9] suggests the the observed mechanosensitivity of neuralization may generalize to many different types of hPSCs.

We and others have previously shown that ECM stiffness can modulate adult neural stem cell (aNSC) differentiation into neurons, astrocytes, and oligodendrocytes[12, 23], and the use of hPSCs in this study allows investigation of progenitor cells representative of earlier developmental periods. Culturing hPSCs on soft ECMs that mimic the stiffness of neural tissue (~100–1500 Pa) promoted the generation of neurons as it did with aNSCs. However, in contrast to the alteration of neuronal lineage commitment observed for aNSCs, for hPSCs the stiffness effect was mediated by increasing the percentage of early (SOX1+) neural progenitors. Interestingly, exposure to soft ECMs for only 5 out of a total of 19 days was sufficient to observe the downstream increase in neurons. Implementation of this “stiffness pulse” strategy thus reveals that *when* a signal is presented may be just as important as *what* signal is presented. Given that mechanical properties can function during multiple stages of differentiation, from neural conversion of hPSCs to neuronal differentiation and maturation of aNSCs, stem cell differentiation protocols that rely primarily on soluble media conditions[1b] could be further improved by designing an optimal and temporally dynamic biophysical microenvironment. Our findings can therefore be applied to engineer biomaterials scaffolds and bioreactors for human pluripotent stem cell differentiation.

Future work could investigate extension of these observations to non-neural lineages, as well as address potential mechanisms responsible for our observations. In our system, softer ECMs resulted in lower extents of cell and colony spreading but did not affect hPSC proliferation or colony formation. The resulting higher effective cell densities or packing may yield smaller and more condensed individual cells and nuclei, as well as impact both the quantity and quality of cell-cell contacts during subsequent cell differentiation. These factors may in turn invoke cell and nuclear size/shape mechanisms important in mesenchymal stem cell differentiation[20c, 24] and/or cell packing/density effects found in hESC systems[25]. It is interesting to note that, while Chambers and colleagues observed a bias in downstream neuronal subtype specification and neural patterning due to cell density/packing[1a], we instead observed an earlier bias in the generation of neural progenitors and early neural ectoderm, suggesting that different combinations of cell-cell contacts, cell density/packing, and/or perhaps cell/nuclear shape may play important roles throughout neurogenesis.

The shape of a cell has been shown to affect its mechanical properties[20c], and ECM stiffness may also directly modulate cellular mechanics, either or both of which could in turn affect neural differentiation. Due to low survival of single hPSCs and inefficient clonal growth[26], it is difficult to study the effects of ECM stiffness directly on single cells. However, intracellular probes of force generation and mechanical properties[2728], in conjunction with biochemical and genetic studies, may help elucidate mechanisms of mechanosensitive hPSC differentiation into neural lineages.

Conclusion

We have shown that hPSC self-renewal is insensitive to ECM stiffness, yet neural differentiation is mechanosensitive. Furthermore, only an early, short stiffness pulse is required to enhance downstream neuronal differentiation. In addition to providing potential mechanistic insights into the mechanosensitive neural differentiation of hPSCs, the short temporal window of exposure to soft ECMs required to improve neurogenesis is important from a technological perspective in the design of cell culture systems. The early mechanosensitivity of hPSCs shown here may thus not only influence the future design parameters of biomaterials to improve the generation of therapeutically relevant cell populations such as dopaminergic neurons, but also inform our understanding of the influence of biophysical cues in early embryonic development.

Experimental

Stem Cell Culture

hPSCs were cultured on Matrigel-coated (BD Biosciences, Franklin Lakes, NJ) tissue culture-treated polystyrene plates and glass chamber wells. For growth or self-renewal conditions, H1 hESCs[9] were cultured in XVIVO media (Lonza, Basel, Switzerland) supplemented with 80 ng/mL human basic fibroblast growth factor (hbFGF, Peprotech, Rocky Hill, NJ) and 0.5 ng/mL transforming growth factor β1 (TGF-β1, R&D Systems, Minneapolis, MN). MSC-iPS hiPSCs[21c] were cultured in mTeSR media with 1× final dilution of mTeSR 5× Supplement (Stemcell Technologies, Vancouver, BC).

Neuronal differentiation conditions were adapted from Chambers et. al.[1a]. Briefly, ~25–50 cell clusters of hPSCs were seeded on ECMs of defined stiffnesses or polystyrene at a total cell density of 25000 cells/cm^2. hPSCs were cultured for 3 days in growth conditions. Differentiation was then induced on day 0 by changing media to DMEM:F12 (Invitrogen, Carlsbad, CA), 20 % knockout serum replacement (KSR, Invitrogen), 0.1 mM β-mercaptoethanol (Sigma-Aldrich, St Louis, MO), 1 μM LDN-193189 (Stemgent, San Diego,

CA), 10 μM SB-451542 (Tocris Biosciences, Ellisville, MO). Half-media changes were made daily from day 1–4. On day 5, cells were either maintained on their current ECM or passed *en bloc* to polystyrene. Media was changed to DMEM:F12, 15 % KSR, 0.25 % N2 supplement (Invitrogen), 0.1 mM β-mercaptoethanol, and 200 ng/mL recombinant N-terminal human sonic hedgehog (SHH) with a C24II Substitution (SHH, R&D Systems). On day 7, media was changed to DMEM:F12, 10 % KSR, 0.5 % N2 supplement, 0.1 mM β-mercaptoethanol, and 200 ng/mL SHH. On day 9, all cells were passed *en bloc* to polystyrene. Medium was changed to DMEM:F12, 5 % KSR, 0.75 % N2 supplement, 0.1 mM β-mercaptoethanol, 200 ng/mL SHH, 100 ng/mL recombinant human fibroblast growth factor-8b (FGF-8b, Peprotech), 20 ng/mL brain-derived neurotrophic factor (BDNF, Peprotech), and 0.2 mM ascorbic acid (Sigma). On day 12, medium was changed to DMEM:F12, 0.1 % N2 supplement, 0.1 mM β-mercaptoethanol, 20 ng/mL BDNF, 0.2 mM ascorbic acid, 20 ng/mL glial-derived neurotrophic factor (GDNF, Peprotech), 1 ng/mL transforming growth factor β3 (TGF-β3, Peprotech), and 1 μM cyclic adenosine monophosphate (Sigma). Medium was changed every two days until day 19. A hemocytometer was used to quantify cell number density per cell culture surface area.

Flow Cytometry Analysis

Cells were dissociated with 0.25% Trypsin/2.5mM EDTA and stained using the following primary antibodies: rabbit anti-Nanog (1:250 dilution; Abcam, Cambridge, UK), mouse anti-Stage-specific embryonic antigen-4 (SSEA-4, 10 μg/mL; Millipore, Billerica, MA), mouse anti-Tra-1-60 FITC conjugate (1:100 dilution; Millipore), mouse anti-Oct-3/4 (1:200 dilution; Santa Cruz Biotechnology, Santa Cruz, CA). Secondary antibodies were FITC-conjugated goat anti-rabbit IgG and Cy5-conjugated goat anti-mouse IgG at a dilution of 1:250 (all from Jackson ImmunoResearch Laboratories Inc., West Grove, PA). Samples were analyzed on a FC500 Analyzer (Beckman-Coulter, Brea, CA).

Immunofluorescence Staining and Microscopy

Cells were fixed with 4% paraformaldehyde. Samples were blocked and permeabilized in 2% goat serum (Sigma) and 0.3% Triton X-100 (Calbiochem, San Diego, CA) in pH 7.4 phosphate buffered solution at room temperature. Samples were incubated for 36 hours at 4°C with the following primary antibodies: mouse anti-β-tubulin III (TUJ1, 1:1000 dilution; Sigma-Aldrich), rabbit anti-tyrosine hydroxylase (TH, 1:1000 dilution; Pel-Freez, Rogers, AR), and rabbit anti-PAX6 (PAX6, 1:250 dilution; Covance, Emeryville, CA). The primary antibody solution was removed, and cells were rinsed and incubated for 2 hours with the secondary antibodies FITC-conjugated goat anti-rabbit IgG and Cy5-conjugated goat anti-mouse IgG at a dilution of 1:250 (all from Jackson ImmunoResearch Laboratories Inc., West Grove, PA). Nuclei were stained with DAPI (Invitrogen) at 10 μg/ml. Cells were manually scored as positive or negative for lineage markers using the optical fractionator method in an unbiased stereological microscope (Zeiss Axio Imager, software by MicroBrightfield). 3–6 experiments were performed in parallel cultures for each study. 15–20 confocal images obtained on a LSM710 (Carl Zeiss Inc, Oberkochen, Germany) were z-stacked and flattened in ImageJ. Additional immunofluorescence and phase images were collected on a Nikon Eclipse TE2000-E microscope with a Photometrics Coolsnap HQ2 camera. Colony sizes were quantified in ImageJ using manual outlining.

Quantitative real time Polymerase Chain Reaction (QRT-PCR)

Cells were lysed and frozen in TRIZOL (Invitrogen), and mRNA was extracted and reverse transcribed to cDNA using the ThermoScript™ RT-PCR System for First-Strand cDNA Synthesis (Invitrogen, Carlsbad, CA). Equivalent amounts of total RNA were transcribed into cDNA, which was subsequently used as template for each QRT-PCR reaction (utilizing a Bio-Rad Laboratories iCycler 5, Hercules, CA). To normalize any remaining variations in

starting cDNA amounts, each reaction was referenced to ribosomal 18S detected using Cal-dye TaqMan probes and the lineage marker was detected using FAM-dye TaqMan probes (Biosearch Technologies, Novato, CA) or Sybr Green (Invitrogen). QRT-PCR reactions were run for each biological sample with n=4–6 for each condition. The TaqMan probes used are listed as follows: (TUJ1, 5'-GCATGGACGAGATGGAGTTCACC-3', 5'-CGACTCCTCCTCGTCGTCTTCGTAC-3', 5'-FAM490-TGAACGACCTGGTGTCCGAG-BHQ-3'), and (18S, 5'-GTAACCCGTTGAACCCCATTC-3', 5'-CCATCCAATCGGTAGTAGCGA-3', 5'-CAL610-AAGTGCGGGTCATAAGCTTGCG-BHQ-3'). PAX6 and SOX1 gene expression was assayed using Qiagen Quantitect Primer Assays (Hs_PAX6_1_SG QT00071169, Hs_SOX1_2_SG QT01008714).

Polyacrylamide Substrate Preparation and Mechanical Characterization

Using a protocol similar to that described previously[5c], 25 mm glass coverslips were cleaned and treated by incubation in 0.1 N NaOH for 1 hour. Coverslips were dipped in 3-aminopropytrimethoxysilane, rinsed with distilled water, the incubated with 0.5% glutaraldehyde for 45 min, shaking at room temperature. Acrylamide/Bisacrylamide solutions were made according to the formulations below:

AA %	BIS %	40% Acrylamide (mL)	2% BIS (mL)	water (mL)	Measured AFM Elastic Modulus (Pa)
3	0.025	3	0.5	36.5	102
4	0.05	4	1	35	692
10	0.3	10	6	24	72904

Tetraethylenediamine was added at 1:1000 and 10% ammonium persulfate was added at 1:100 to catalyze the polymerization reaction. 40 μL (for 70 μm final nominal thickness) of the polymerizing solution was added to a clean glass slide. The treated coverslips were placed on top of the polymerizing solution to create a flat gel that covalently links to the coverslip. 100 μg/ml poly-D-lysine was linked to the gel surface through sulfo-SANPAH (Thermo-Fisher, Waltham, MA) chemistry (both in 200 mM HEPES buffer, pH 8.5) and incubated for 3 hours at 37°C, and 250 μg/ml Matrigel (in phosphate buffered solution, pH 7.5) was then absorbed for 3 hours at 37°C.

An Asylum MFP-3D atomic force microscope (Asylum Research, Santa Barbara, CA) was used to probe material mechanical properties in contact mode. Silicon nitride pyramidal AFM tips (MLCT-ANUM, Veeco Metrology, Inc., Santa Barbara, CA) with spring constants of 10–30 pN/nm were calibrated by the thermal resonance method. All measurements were made at a constant velocity of 2 μm/s. Elastic moduli reported are Young's moduli calculated from force curves using the Hertz model {Domke, 1998 #70} modified for a pyramidal tip geometry {Rosenbluth, 2006 #71} and assuming a Poisson ratio of 0.45. Force curves were fitted only to the first 500 nm of indentation to minimize mechanical contributions from the underlying substrate {Domke, 1998 #70}.

Acknowledgments

We thank William Bretzlaff and Daniela Mehech for technical assistance. This work was supported by a National Defense Science and Engineering Graduate Fellowship and a National Science Foundation Graduate Research Fellowship to A. J. Keung. D. V. Schaffer wishes to acknowledge the support of the CIRM grant RT2-02022 and

CIRM hESC Shared Research Facility award CL1- 00519-1. S. Kumar wishes to acknowledge the support of a UC Berkeley Stem Cell Center Seed Grant, the Arnold and Mabel Beckman Young Investigator Award, a PECASE Award from the Army Research Office (W911NF-09-1-0507), and the NIH Director's New Innovator Award (1DP2OD004213), a part of the NIH Roadmap for Medical Research.

References

1. (a) Chambers SM, Fasano Ca, Papapetrou EP, Tomishima M, Sadelain M, Studer L. Highly efficient neural conversion of human ES and iPS cells by dual inhibition of SMAD signaling. Nature biotechnology. 2009; 27:275–280.(b) Kriks S, Shim J-W, Piao J, Ganat YM, Wakeman DR, Xie Z, Carrillo-Reid L, Auyeung G, Antonacci C, Buch A, Yang L, Beal MF, Surmeier DJ, Kordower JH, Tabar V, Studer L. Dopamine neurons derived from human ES cells efficiently engraft in animal models of Parkinson‚Äôs disease. Nature. 2011; 480:547–551. [PubMed: 22056989]
2. (a) Takahashi K, Tanabe K, Ohnuki M, Narita M, Ichisaka T, Tomoda K, Yamanaka S. Induction of pluripotent stem cells from adult human fibroblasts by defined factors. Cell. 2007; 131:861–872. [PubMed: 18035408] (b) Yu J, Vodyanik Ma, Smuga-Otto K, Antosiewicz-Bourget J, Frane JL, Tian S, Nie J, Jonsdottir Ga, Ruotti V, Stewart R, Slukvin II, Thomson Ja. Induced pluripotent stem cell lines derived from human somatic cells. Science (New York, N.Y.). 2007; 318:1917–1920.
3. Yan Y, Yang D, Zarnowska ED, Du Z, Werbel B, Valliere C, Pearce Ra, Thomson Ja, Zhang S-C. Directed differentiation of dopaminergic neuronal subtypes from human embryonic stem cells. Stem cells (Dayton, Ohio). 2005; 23:781–790.
4. (a) Chen X, Xu H, Yuan P, Fang F, Huss M, Vega VB, Wong E, Orlov YL, Zhang W, Jiang J, Loh Y-H, Yeo HC, Yeo ZX, Narang V, Govindarajan KR, Leong B, Shahab A, Ruan Y, Bourque G, Sung W-K, Clarke ND, Wei C-L, Ng H-H. Integration of external signaling pathways with the core transcriptional network in embryonic stem cells. Cell. 2008; 133:1106–1117. [PubMed: 18555785] (b) Desbordes SC, Placantonakis DG, Ciro A, Socci ND, Lee G, Djaballah H, Studer L. High-throughput screening assay for the identification of compounds regulating self-renewal and differentiation in human embryonic stem cells. Cell stem cell. 2008; 2:602–612. [PubMed: 18522853] (c) Loh Y-H, Yang L, Yang JC, Li H, Collins JJ, Daley GQ. Genomic Approaches to Deconstruct Pluripotency. Annual review of genomics and human genetics. 2010
5. (a) Engler AJ, Sen S, Sweeney HL, Discher DE. Matrix elasticity directs stem cell lineage specification. Cell. 2006; 126:677–689. [PubMed: 16923388] (b) Fu J, Wang Y-k, Yang MT, Desai Ra, Yu X, Liu Z, Chen CS. Mechanical regulation of cell function with geometrically modulated elastomeric substrates. Nature methods. 2010; 7:733–736. [PubMed: 20676108] (c) Keung AJ, de Juan-Pardo EM, Schaffer DV, Kumar S. Rho GTPases Mediate the Mechanosensitive Lineage Commitment of Neural Stem Cells. Stem cells (Dayton, Ohio). 2011:1886–1897.
6. (a) Chowdhury F, Li Y, Poh Y-C, Yokohama-Tamaki T, Wang N, Tanaka TS. Soft substrates promote homogeneous self-renewal of embryonic stem cells via downregulating cell-matrix tractions. PloS one. 2010; 5:e15655–e15655. [PubMed: 21179449] (b) Chowdhury F, Na S, Li D, Poh Y-C, Tanaka TS, Wang F, Wang N. Material properties of the cell dictate stress-induced spreading and differentiation in embryonic stem cells. Nature materials. 2009; 9:82–88.
7. Brons IGM, Smithers LE, Trotter MWB, Rugg-Gunn P, Sun B, Chuva de Sousa Lopes SM, Howlett SK, Clarkson A, Ahrlund-Richter L, Pedersen Ra, Vallier L. Derivation of pluripotent epiblast stem cells from mammalian embryos. Nature. 2007; 448:191–195. [PubMed: 17597762]
8. Saha S, Ji L, de Pablo JJ, Palecek SP. Inhibition of human embryonic stem cell differentiation by mechanical strain. Journal of cellular physiology. 2006; 206:126–137. [PubMed: 15965964]
9. Thomson, Ja. Embryonic Stem Cell Lines Derived from Human Blastocysts. Science. 1998; 282:1145–1147. [PubMed: 9804556]
10. Wei CL, Miura T, Robson P, Lim S-K, Xu X-Q, Lee MY-C, Gupta S, Stanton L, Luo Y, Schmitt J, Thies S, Wang W, Khrebtukova I, Zhou D, Liu ET, Ruan YJ, Rao M, Lim B. Transcriptome profiling of human and murine ESCs identifies divergent paths required to maintain the stem cell state. Stem cells (Dayton, Ohio). 2005; 23:166–185.
11. (a) Evans ND, Minelli C, Gentleman E, LaPointe V, Patankar SN, Kallivretaki M, Chen X, Roberts CJ, Stevens MM. Substrate stiffness affects early differentiation events in embryonic stem cells. European cells & materials. 2009; 18:1–13. discussion 13-4; [PubMed: 19768669] (b) Zoldan J, Karagiannis ED, Lee CY, Anderson DG, Langer R, Levenberg S. The influence of scaffold

elasticity on germ layer specification of human embryonic stem cells. Biomaterials. 2011; 32:9612–9621. [PubMed: 21963156]

12. Saha K, Keung AJ, Irwin EF, Li Y, Little L, Schaffer DV, Healy KE. Substrate modulus directs neural stem cell behavior. Biophysical journal. 2008; 95:4426–4438. [PubMed: 18658232]
13. Flanagan LA, Ju YE, Marg B, Osterfield M, Janmey PA. Neurite branching on deformable substrates. Neuroreport. 2002; 13:2411–2411. [PubMed: 12499839]
14. (a) Nichols J, Smith A. Naive and primed pluripotent states. Cell stem cell. 2009; 4:487–492. [PubMed: 19497275] (b) Tesar PJ, Chenoweth JG, Brook FA, Davies TJ, Evans EP, Mack DL, Gardner RL, McKay RD. New cell lines from mouse epiblast share defining features with human embryonic stem cells. Nature. 2007; 448:196–199. [PubMed: 17597760]
15. Goke J, Jung M, Behrens S, Chavez L, O'Keeffe S, Timmermann B, Lehrach H, Adjaye J, Vingron M. Combinatorial binding in human and mouse embryonic stem cells identifies conserved enhancers active in early embryonic development. PLoS Comput Biol. 2011; 7 e1002304.
16. Koestenbauer S, Zech NH, Juch H, Vanderzwalmen P, Schoonjans L, Dohr G. Embryonic stem cells: similarities and differences between human and murine embryonic stem cells. Am J Reprod Immunol. 2006; 55:169–180. [PubMed: 16451351]
17. Xie CQ, Jeong Y, Fu M, Bookout AL, Garcia-Barrio MT, Sun T, Kim BH, Xie Y, Root S, Zhang J, Xu RH, Chen YE, Mangelsdorf DJ. Expression profiling of nuclear receptors in human and mouse embryonic stem cells. Mol Endocrinol. 2009; 23:724–733. [PubMed: 19196830]
18. Maurer J, Nelson B, Cecena G, Bajpai R, Mercola M, Terskikh A, Oshima RG. Contrasting expression of keratins in mouse and human embryonic stem cells. PloS one. 2008; 3:e3451. [PubMed: 18941637]
19. (a) Niwa H, Ogawa K, Shimosato D, Adachi K. A parallel circuit of LIF signalling pathways maintains pluripotency of mouse ES cells. Nature. 2009; 460:118–122. [PubMed: 19571885] (b) Vallier L, Alexander M, Pedersen Ra. Activin/Nodal and FGF pathways cooperate to maintain pluripotency of human embryonic stem cells. Journal of cell science. 2005; 118:4495–4509. [PubMed: 16179608]
20. (a) Du J, Chen X, Liang X, Zhang G, Xu J, He L, Zhan Q, Feng X-Q, Chien S, Yang C. Integrin activation and internalization on soft ECM as a mechanism of induction of stem cell differentiation by ECM elasticity. Proceedings of the National Academy of Sciences of the United States of America. 2011; 108:9466–9471. [PubMed: 21593411] (b) Gao L, McBeath R, Chen CS. Stem cell shape regulates a chondrogenic versus myogenic fate through Rac1 and N-cadherin. Stem cells (Dayton, Ohio). 2010; 28:564–572.(c) McBeath R, Pirone DM, Nelson CM, Bhadriraju K, Chen CS. Cell shape, cytoskeletal tension, and RhoA regulate stem cell lineage commitment. Developmental cell. 2004; 6:483–495. [PubMed: 15068789]
21. (a) Kim K, Doi a, Wen B, Ng K, Zhao R, Cahan P, Kim J, Aryee MJ, Ji H, Ehrlich LIR, Yabuuchi a, Takeuchi a, Cunniff KC, Hongguang H, McKinney-Freeman S, Naveiras O, Yoon TJ, Irizarry Ra, Jung N, Seita J, Hanna J, Murakami P, Jaenisch R, Weissleder R, Orkin SH, Weissman IL, Feinberg aP, Daley GQ. Epigenetic memory in induced pluripotent stem cells. Nature. 2010; 467:285–290. [PubMed: 20644535] (b) Kim K, Zhao R, Doi A, Ng K, Unternaehrer J, Cahan P, Hongguang H, Loh Y-H, Aryee MJ, Lensch MW, Li H, Collins JJ, Feinberg AP, Daley GQ. Donor cell type can influence the epigenome and differentiation potential of human induced pluripotent stem cells. Nature Biotechnology. 2011; 29:1117–1119.(c) Park, I-h; Zhao, R.; West, Ja; Yabuuchi, A.; Huo, H.; Ince, Ta; Lerou, PH.; Lensch, MW.; Daley, GQ. Reprogramming of human somatic cells to pluripotency with defined factors. Nature. 2008; 451:141–146. [PubMed: 18157115]
22. Narsinh KH, Plews J, Wu JC. Comparison of human induced pluripotent and embryonic stem cells: fraternal or identical twins? Mol Ther. 2011; 19:635–638. [PubMed: 21455209]
23. (a) Leipzig ND, Shoichet MS. The effect of substrate stiffness on adult neural stem cell behavior. Biomaterials. 2009; 30:6867–6878. [PubMed: 19775749] (b) Teixeira AI, Ilkhanizadeh S, Wigenius Ja, Duckworth JK, Inganvßs O, Hermanson O. The promotion of neuronal maturation on soft substrates. Biomaterials. 2009; 30:4567–4572. [PubMed: 19500834]
24. Pajerowski JD, Dahl KN, Zhong FL, Sammak PJ, Discher DE. Physical plasticity of the nucleus in stem cell differentiation. Proceedings of the National Academy of Sciences. 2007; 104:15619–15619.

25. Bauwens, ClL; Peerani, R.; Niebruegge, S.; Woodhouse, Ka; Kumacheva, E.; Husain, M.; Zandstra, PW. Control of human embryonic stem cell colony and aggregate size heterogeneity influences differentiation trajectories. Stem cells (Dayton, Ohio). 2008; 26:2300–2310.

26. Watanabe K, Ueno M, Kamiya D, Nishiyama A, Matsumura M, Wataya T, Takahashi JB, Nishikawa S, Nishikawa S-i, Muguruma K, Sasai Y. A ROCK inhibitor permits survival of dissociated human embryonic stem cells. Nature biotechnology. 2007; 25:681–686.

27. Grashoff C, Hoffman BD, Brenner MD, Zhou R, Parsons M, Yang MT, McLean Ma, Sligar SG, Chen CS, Ha T, Schwartz Ma. Measuring mechanical tension across vinculin reveals regulation of focal adhesion dynamics. Supplementals. Nature. 2010; 466:263–266. [PubMed: 20613844]

28. Wirtz D. Particle-tracking microrheology of living cells: principles and applications. Annual review of biophysics. 2009; 38:301–326.

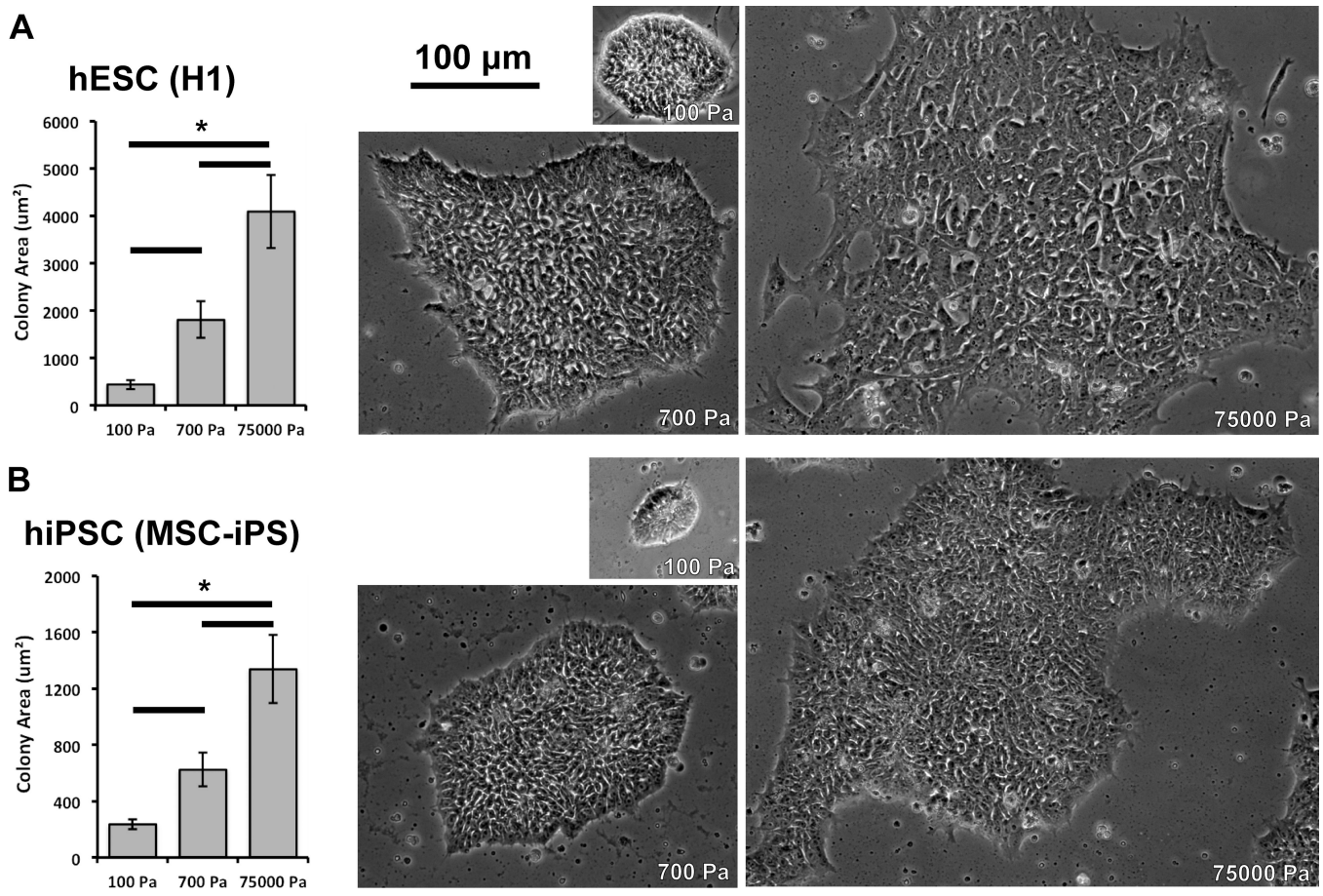

Figure 1.

hPSC colony area increases with substrate stiffness. Quantification of colony area and phase contrast images of human (A) embryonic H1 and (B) induced pluripotent MSC-iPS stem cells cultured on 100, 700, and 75000 Pa polyacrylamide substrates after 3 days in self-renewal conditions. Error bars are 95% confidence intervals, $n = 220–300$ colonies. $*p < .05$ (ANOVA, Tukey-Kramer). Abbreviations: ANOVA, analysis of variance; MSC-iPS, mesencymal stem cell-induced pluripotent stem cell; hPSC, human pluripotent stem cell; hESC, human embryonic stem cell; hiPSC, human induced pluripotent stem cell.

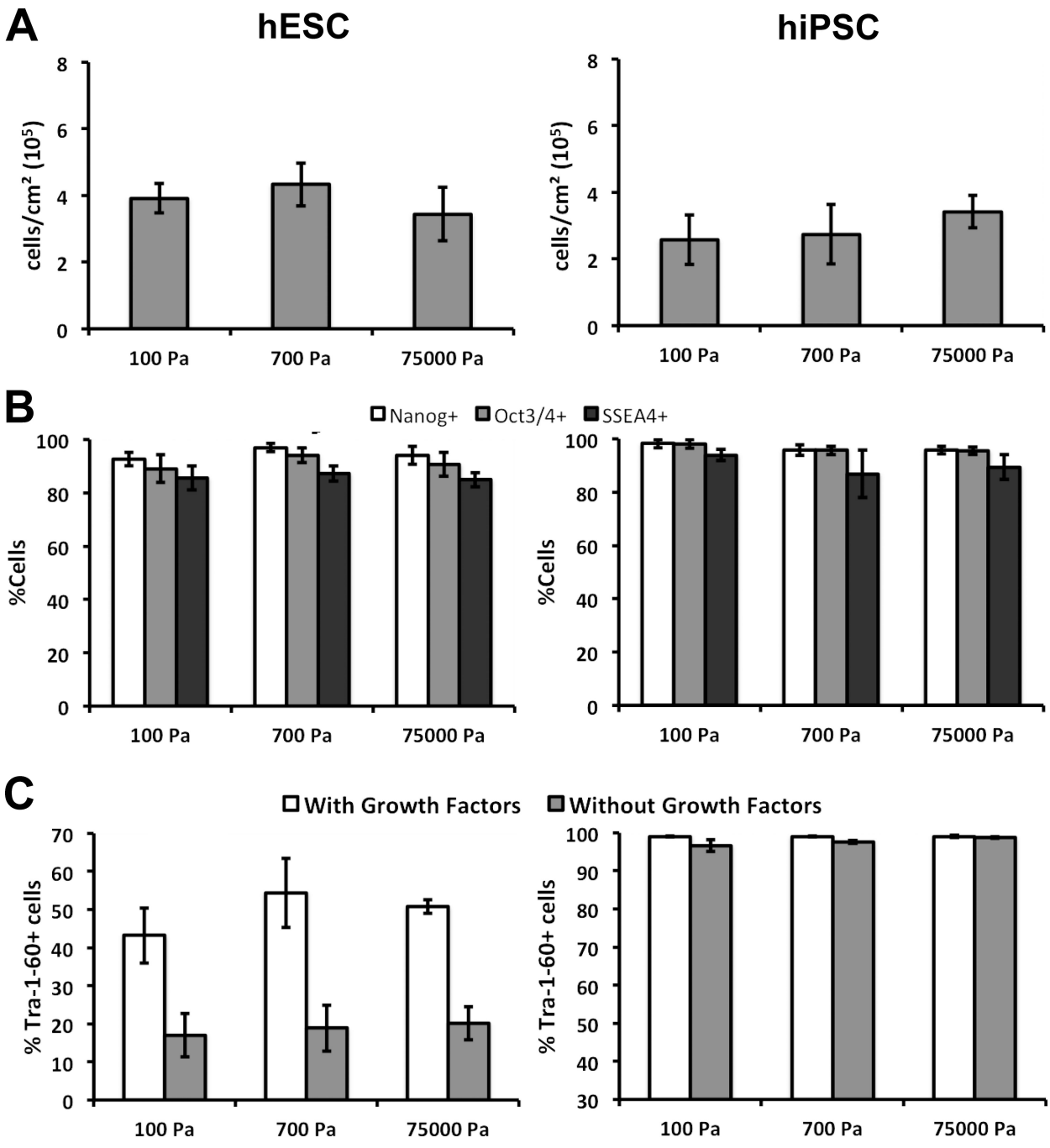

Figure 2.

hPSC pluripotency marker expression is not altered by substrate stiffness. hESCs (left) and hiPSCs (right) show similar (A) cell numbers per cell culture surface area and (B) expression of pluripotency markers after 3 days in self-renewal conditions. (C) Substrate stiffness does not alter the expression of pluripotency marker Tra-1-60 even with the withdrawal of growth factors. Error bars are 95% confidence intervals, $n = 3$. $^{*}p < .05$ (ANOVA, Tukey-Kramer). Abbreviations: ANOVA, analysis of variance; hESC, human embryonic stem cell; hiPSC, human induced pluripotent stem cell.

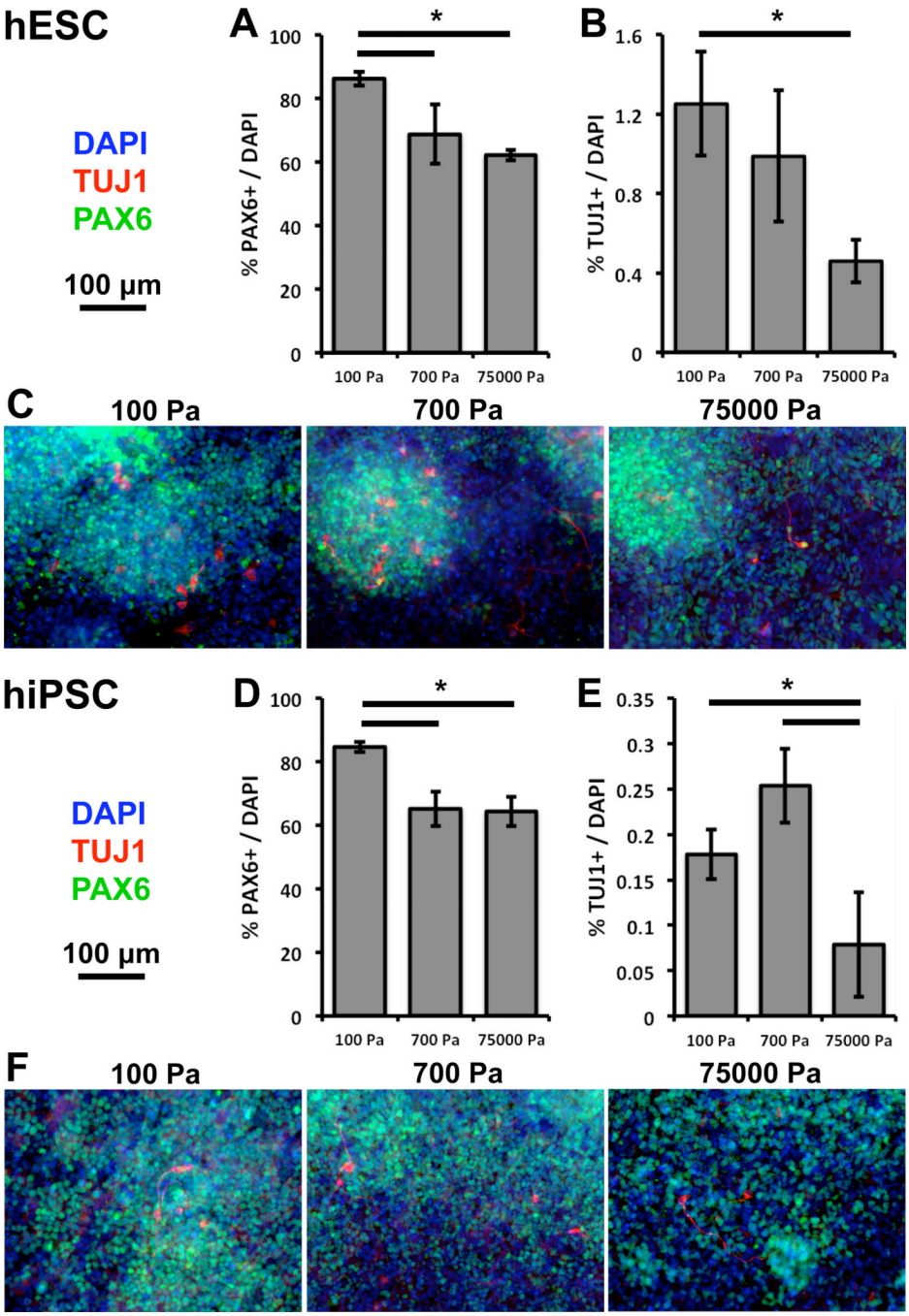

Figure 3.

Softer substrates promote neural ectodermal and neuronal differentiation from hPSCs after 9 days of differentiation. Compared to 700 and 75000 Pa substrates, 100 Pa substrates promote PAX6 gene expression in cultures derived from (A) hESCs and (D) hiPSCs. Compared to 75000 Pa substrates, 100 and 700 Pa substrates promote neuronal marker TUJ1 gene expression from cultures derived from (B) hESCs and (E) hiPSCs. Representative immunofluorescence images of cultures derived from (C) hESCs and (F) hiPSCs. Red-TUJ1, Green-PAX6, Blue-DAPI. Error bars are 95% confidence intervals, $n = 3$. *$p < .05$ (ANOVA, Tukey-Kramer). Abbreviations: ANOVA, analysis of variance; hPSC, human

pluripotent stem cell; hESC, human embryonic stem cell; hiPSC, human induced pluripotent stem cell.

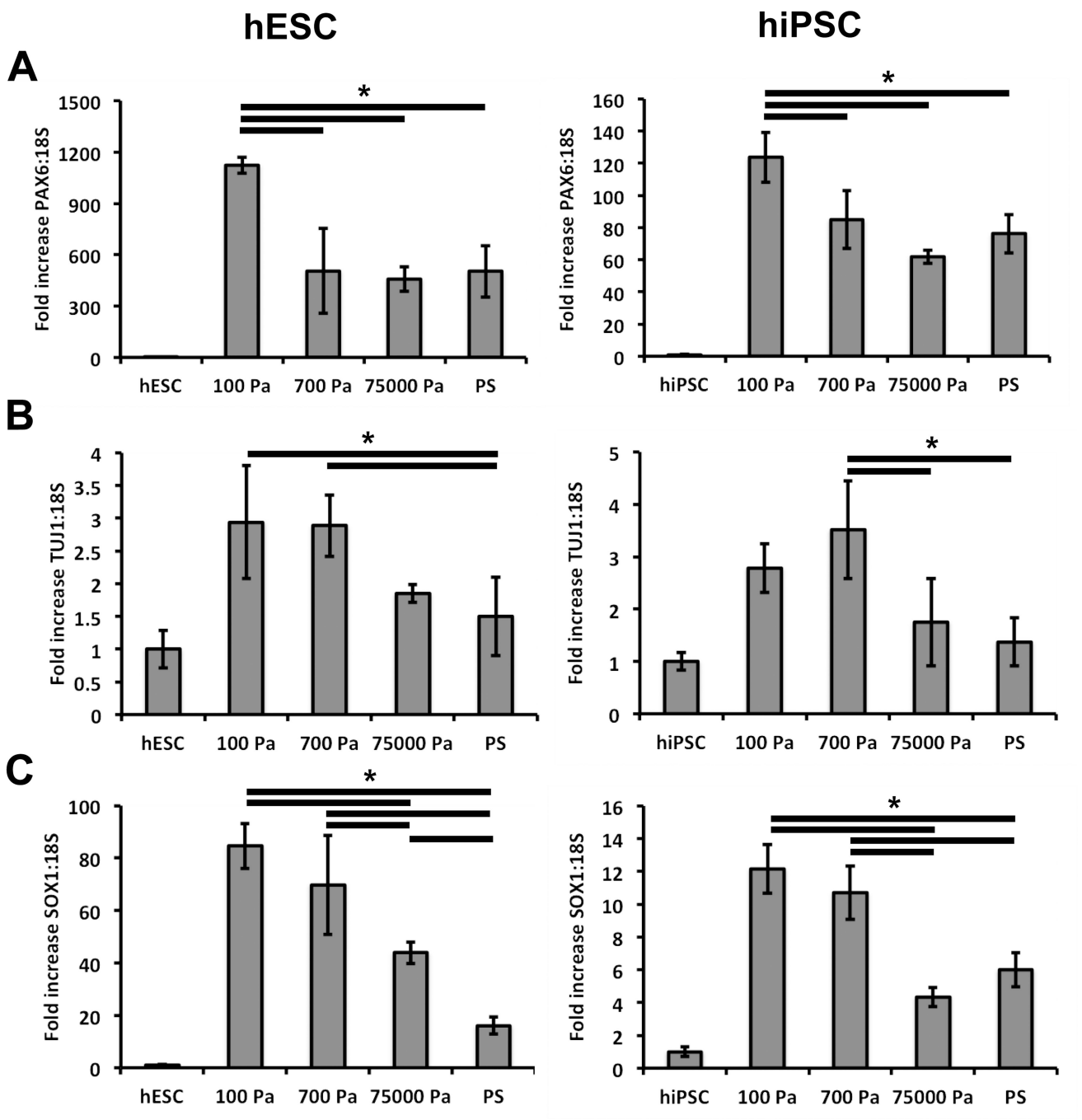

Figure 4.

Softer substrates promote neuronal and early ectodermal differentiation from hPSCs after 9 days in culture. (A) 100 Pa substrates promote PAX6 gene expression in (left) hESCs and (right) hiPSCs. (B) 100 and 700 Pa substrates promote TUJ1 gene expression in hPSCs. (C) 100 and 700 Pa substrates promote SOX1 gene expression in hPSCs. Error bars are 95% confidence intervals, $n = 4$. *$p < .05$ (ANOVA, Tukey-Kramer). Abbreviations: ANOVA, analysis of variance; hPSC, human pluripotent stem cell; hESC, human embryonic stem cell; hiPSC, human induced pluripotent stem cell; PS, polystyrene.

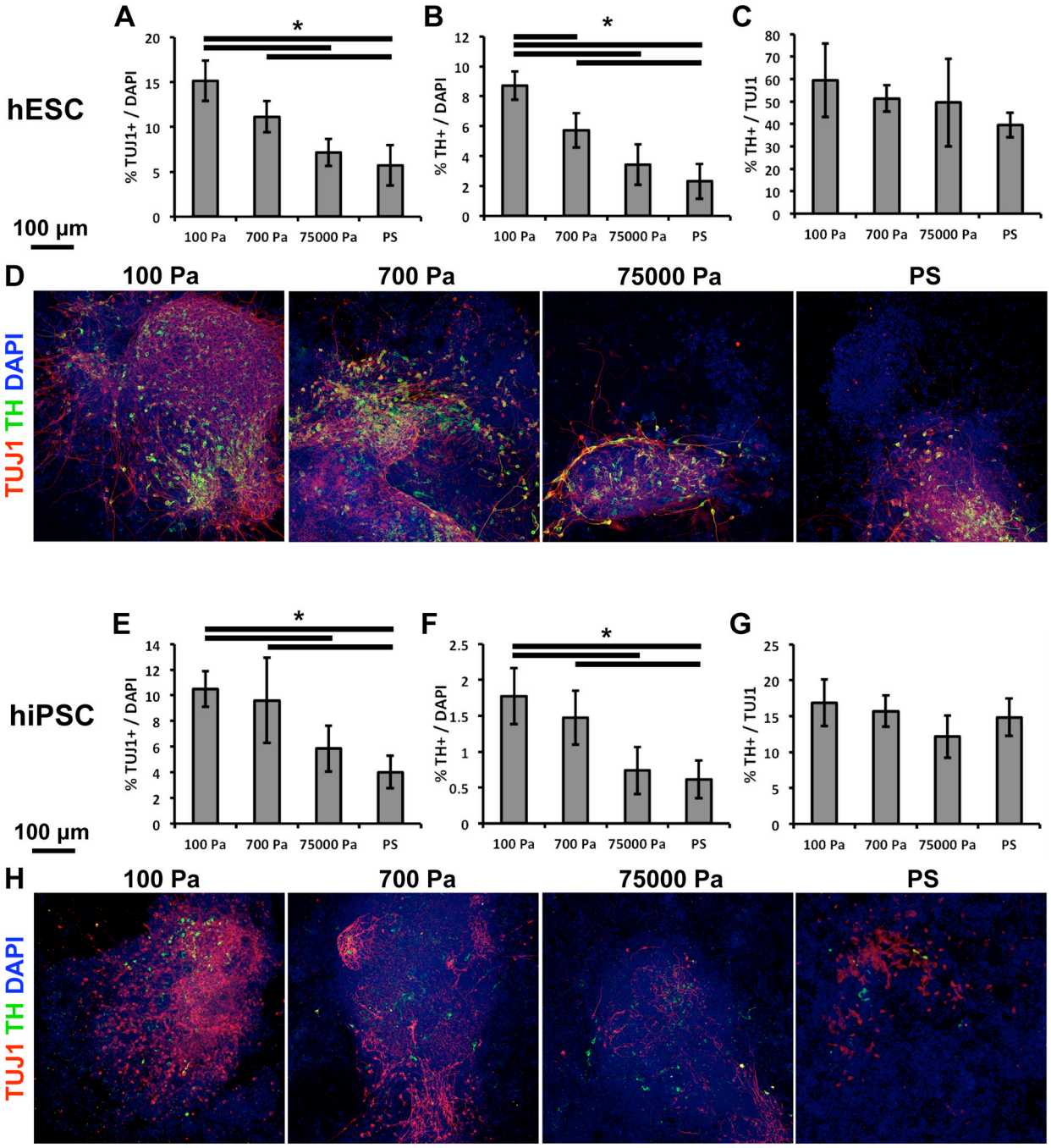

Figure 5.

Softer substrates promote the differentiation of hPSCs into neurons and dopaminergic neurons but do not change the proportion of dopaminergic to total neurons after 19 days of differentiation. The percentage of cells (DAPI+) that are TUJ1+ (A-hESC, E-hiPSC) and TH + (B-hESC, F-hiPSC) decreases with increasing substrate stiffness. The percentage of TUJ1+ cells that are also TH+ does not change with substrate stiffness (C-hESC, G-hiPSC). Representative immunofluorescence images of cultures derived from (D) hESCs and (H) hiPSCs. Red-TUJ1, Green-TH, Blue-DAPI. Error bars are 95% confidence intervals, $n = 4$. *$p < .05$ (ANOVA, Tukey-Kramer). Abbreviations: ANOVA, analysis of variance; hPSC,

human pluripotent stem cell; hESC, human embryonic stem cell; hiPSC, human induced pluripotent stem cell; PS, polystyrene.

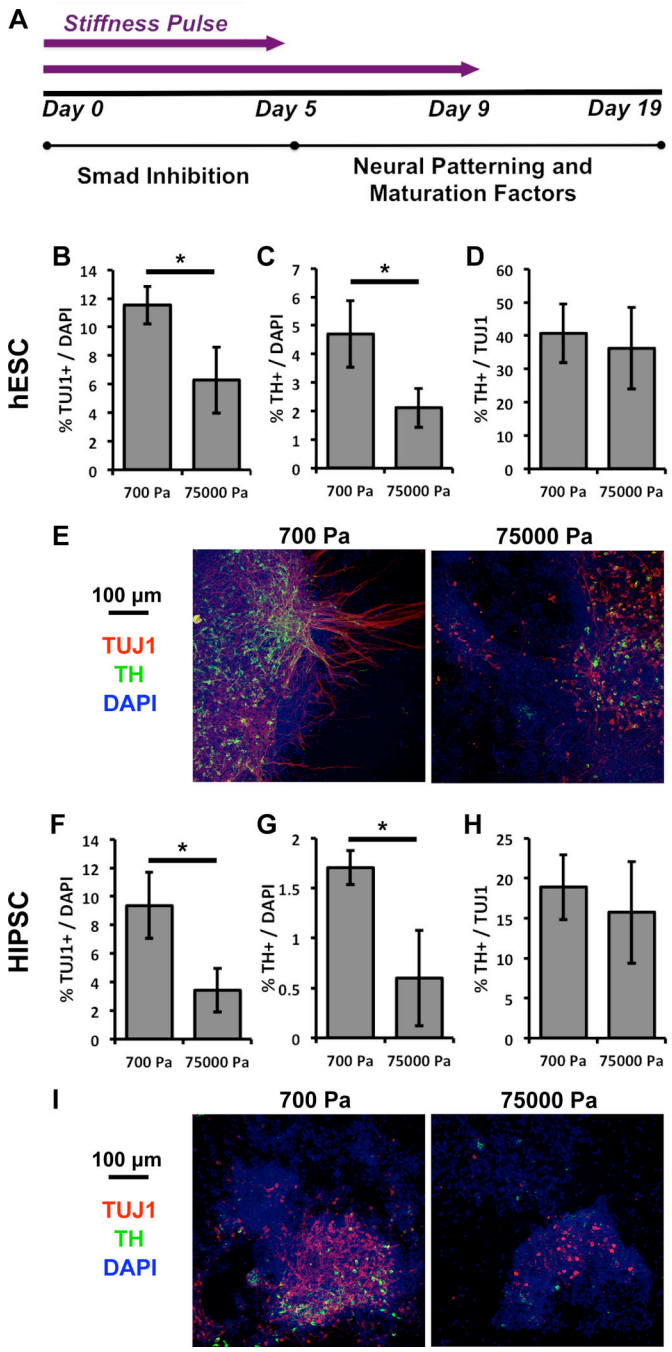

Figure 6.

An early substrate stiffness signal is sufficient to recapitulate the full differentiation phenotypes of hPSCs. (A) A shortened substrate stiffness pulse (from 9 to 5 days) prior to neural patterning is sufficient to modulate neuronal and dopaminergic differentiation to the same extent as a 9 day pulse. The percentage of cells (DAPI+) that are TUJ1+ (B-hESC, F-hiPSC) and TH+ (C-hESC, G-hiPSC) decreases with increasing substrate stiffness. The ratio of TH+ to TUJ1+ cells does not change with substrate stiffness (D-hESC, H-hiPSC). Representative immunofluorescence images of cultures derived from (E) hESCs and (I) hiPSCs. Red-TUJ1, Green-TH, Blue-DAPI. Error bars are 95% confidence intervals, $n = 4$.

*$p < .05$ (ANOVA, Tukey-Kramer). Abbreviations: ANOVA, analysis of variance; hESC, human embryonic stem cell; hiPSC, human induced pluripotent stem cell; PS, polystyrene.